



ELSEVIER

Biochimica et Biophysica Acta 1452 (1999) 89–102



www.elsevier.com/locate/bba

Centric diatom morphogenesis: a model based on a DLA algorithm investigating the potential role of microtubules

John Parkinson ^{a,*}, Yves Brechet ^b, Richard Gordon ^c

^a *Edinburgh centre for Protein Technology, Department of Chemistry, University of Edinburgh, Kings Buildings, West Mains Road, Edinburgh EH9 3JJ, UK*

^b *Laboratoire de Thermodynamique et Physico-Chimie Metallurgiques, ENSEEG, 1130 Rue de la Piscine, Domaine Universitaire, BP 75, 38402 Saint-Martin-D'Herès Cedex, France*

^c *Department of Radiology, Health Sciences Center, 820 Sherbrook Street, Winnipeg, Man., Canada*

Received 18 May 1999; received in revised form 2 August 1999; accepted 16 August 1999

Abstract

Diatoms are single-celled algae which possess characteristic rigid cell walls (frustules) composed of amorphous silica. Frustule formation occurs within a specialised organelle termed the silica deposition vesicle (SDV). During diatom morphogenesis, silica particles are transported to the SDV by silica transport vesicles. Once released within the SDV, the particles are then thought to diffuse until they encounter part of the growing aggregate upon which they adhere. The particles may then undergo a further period of surface relocalisation (sintering) which leads to a smoothing of the surface. A number of computer simulations based on a modified diffusion-limited aggregation (DLA) algorithm, have been undertaken to investigate the potential role of microtubules (which are known to be associated with the periphery of the SDV) in localising deposition of new siliceous material. Based on our findings, we present a new model of diatom morphogenesis which is able to account for many morphological features of diatoms including the influence of environmental effects such as changes in pH and salinity, and the formation of a regular branched pattern. © 1999 Elsevier Science B.V. All rights reserved.

Keywords: Diatom; Morphogenesis; Diffusion-limited aggregation; Computer simulation; Microtubule

1. Introduction

Diatoms are single-celled eukaryotic algae responsible for about 25% of the world's net primary pro-

duction [1]. They possess a characteristically rigid cell wall (termed a frustule) composed of silica. Diatom frustules consist of two usually nearly identical halves (valves) which fit together like the bottom and cover of a petri-dish, enclosing the cell. There are currently estimated to be over 100 000 different species classified by their unique frustule morphologies [2]. Diatoms may be split into two main groups depending upon the symmetry of their frustules. Centric diatoms tend to be radially symmetric whilst pennate diatoms tend to be elongated and generally have parallel striae (furrows or rows of holes in the silica) arranged normal to the long axis.

Abbreviations: SDV, silica deposition vesicle; STV, silica transport vesicle; DLA, diffusion-limited aggregation; K , a tunable parameter used to represent surface tension; T , a tunable parameter relating to temperature; X , a tunable parameter used to represent surface mobility; R_{\max} , distance of the furthest point of the growing aggregate from its centre

* Corresponding author;

E-mail: john.parkinson@chem.ed.ac.uk

The process of frustule formation is not well understood but is thought to involve the diffusion-limited precipitation of silica within a specialised organelle termed the silica deposition vesicle (SDV) [3]. Amorphous silica particles of relatively low molecular mass (approximately 1–10 nm in diameter) are thought to be transported to the periphery of the SDV by silica transport vesicles (STVs) [4]. Once released inside the SDV, the particles presumably diffuse until they encounter part of the growing aggregate upon which they adhere. The surface of the particles is thought to consist mainly of silanol groups [5] ($=\text{Si}(\text{OH})_2$ or $\equiv\text{Si}-\text{OH}$) which enable them to diffuse over the surface of the aggregate in a process termed sintering [3]. This surface migration allows the molecules to re-organise their positions towards a thermodynamic equilibrium, usually resulting in a smoothing of the aggregate surface. Growth of the frustule then proceeds by the further release of new material. Sintering is linked with the phenomenon of Oswald ripening [6] and appears to be dependent upon both pH and salt concentration [7,8] (for an explanation of Oswald ripening see Section 2). This may explain the changes in frustule morphologies observed when a single diatom species is grown under varying conditions [9–11]. After deposition and a period of surface relocalisation, the silica morphology becomes stabilised in a process which may involve a surface inorganic cation such as aluminium. Although little is known about how the silica is transported to the SDV, microtubules have been found to be associated with the lateral margins of the SDV and remain in association as the SDV increases in size (due to accumulation of STVs) [12]. The aim of this study was to attempt to simulate the process of frustule formation in order to further understand the roles of surface diffusion and microtubules in the generation of diatom morphology.

Previous attempts at modelling frustule formation have involved the use of computer simulation of diffusion-limited aggregation (DLA) [3,13]. DLA has been used in a number of studies to model a range of diverse growth phenomena including snowflake formation [14,15], electrolytic deposition [16] and the creation of drainage networks [17]. The complex shapes obtained from these models are typical of out of equilibrium growth processes. However, in gener-

al, DLA algorithms cannot model the morphological stability of these structures with respect to subsequent ageing. Phenomena such as the sintering observed during diatom morphogenesis, require an investigation into the subsequent diffusion of accreted particles over the surface of the aggregate after adsorption. To account for this surface diffusion, the DLA algorithm must be modified to include terms that describe the behaviour of accreted particles.

In this paper we describe a modified version of the basic DLA algorithm which includes these terms and focus on the qualitative consequences on the morphology. The results are displayed using morphology maps which can be readily interpreted in terms of experimental parameters and may therefore be used to predict the consequences of changes in growth conditions for diatom morphogenesis. In addition, the influence of microtubules postulated to be responsible for the localised deposition of new material [3] was also explored. Due to the relative flatness of the SDV (the initial thickness of the SDV is comparable to the diameter of the silica particles diffusing within it [3,18]), the model was simulated in two dimensions.

2. Materials and methods

All simulations were undertaken on a SGI Impact 10000 workstation running IRIX 6.5.3. Programs were written in the C programming language. The model was based on a 2000×2000 hexagonal lattice [19]. An initial nucleus consisting of 61 accreted particles arranged as a solid hexagon was placed at the centre of the lattice. During the growth of the aggregate, new particles were placed on a circular release template of radius $R_{\text{max}} + L$ (where R_{max} is the distance of the furthest point of the growing aggregate from its centre and L was a constant defined at the beginning of the simulation as a number ranging from 1 to 100). Although the initial placement of particles on the release template was random the perimeter, in some simulations, particles were placed at defined release sites (representing the termini of microtubules). After their initial placement, particles were allowed to move at random (diffuse) on the lattice. Note that we are assuming that particles involved in sintering are the same size as precipitating

particles (cf. [3]). In some simulations particle movement was confined to a circle centred on the nucleus of radius $L+P$ (where P is the greatest radius of the precipitate). This feature was incorporated to simulate the SDV membrane, assumed to be circular, being a certain distance from the growing aggregate. After release, the particle was allowed to continue moving until it accreted to the growing cluster after which a new particle was released. For certain simulations, the sites of release were allowed to change their radial position as the aggregate increased in size. This was achieved by altering the angle for the site of release by W radians after the addition of each new particle. W was calculated according to the following formula:

$$W = 0.5 - \text{rand}(1) / (Y \times R_{\max}) \quad (1)$$

where $\text{rand}(1)$ is a function returning a random variable uniformly distributed over the interval (0,1). This feature introduces a new tunable parameter, Y , representing the angular mobility of the microtubule during diatom growth. In addition, the minimum distance separating neighbouring sites of release was controlled. This was achieved by allowing sites of release to alter their radial position only if they did not move closer than R radians to a neighbouring site of release where R is defined as:

$$R = Z / R_{\max} \quad (2)$$

Where Z is a tunable parameter. Note that assigning the value of 0 to Z effectively allows the sites of release to cross over each other.

Since the surface properties of silica particles are important in generating frustule morphology, an attempt at simulating these effects was included in the model. After addition of a new particle to the lattice, particles were picked at random and subjected to a ‘shaking’ algorithm. In this algorithm an empty lattice site neighbouring a particle is chosen at random, and the relative energy states compared. As with typical Monte-Carlo algorithms [20], a particle is given a probability of moving from one lattice site to another depending upon the relative change in energy. The number of such events was determined by the value of a parameter X : if N particles were present on the lattice, the number of shakes between subsequent additions was XN . Physically when the number of particles arriving per unit time on the

lattice is decreasing, it may be simulated by increasing X . The probability, p , of a particle exchanging sites is given by:

$$p(\text{accretion}) = \min(1, e^{-\Delta E/T}) \quad (3)$$

where T is a temperature related term and ΔE represents a change in relative energy based on a particle accreting to a surface of curvature C . The energy term, ΔE , contained both the driving force (in terms of hydrophobic and bond interactions) and the surface tension (a nonlocal term related to the curvature).

$$\Delta E = \Delta E_i + \Delta E_c \quad (4)$$

where ΔE_i is the change in interaction energy between neighbouring particles and ΔE_c is the change in energy related to interface curvature. For the model, ΔE_b was the difference in the number of interparticle bonds (nearest neighbours) between the site where the particle originates and the intended destination site. ΔE_c is related to the change in chemical potential associated with surface curvature (Gibbs–Thomson effect) [21]. This change in chemical potential is inversely proportional to the local radius of curvature. ΔE_c is thus proportional to the difference of local curvature between the site from which the particle originates, $1/R_i$, and the intended site of destination, $1/R_d$.

$$\Delta E_c = \Gamma \times \left(\frac{1}{R_i} - \frac{1}{R_d} \right) \quad (5)$$

Where Γ is the surface tension. From Eq. 5 it is noted that the boundary curvature provides a driving force which causes atoms to move towards the convex side of an interface. This results in small precipitates becoming smaller and large precipitates increasing in size, a phenomenon known as Oswald ripening [6].

In order to determine this curvature, which is in effect a continuum differential concept, on a discrete lattice we have used the following method. The curvature term for a particle at the surface of an aggregate was obtained by evaluating the proportion of occupied sites within a hexagon, containing 61 lattice units, centred on the particle being moved. A hexagon was chosen in order to simplify and reduce computational time. It was found that the size of the hexagon had little effect on the range of morpholo-

gies provided that it was large enough to determine the local curvature (results not shown). In the continuum limit around a flat interface, the proportion of occupied sites should be 0.5, less than 0.5 for positive curvature and greater than 0.5 for negative curvature. A good estimate, M , for the relative curvature is therefore:

$$M = 0.5 - \% \text{ occupied sites} \quad (6)$$

The capillary energy can therefore be estimated by:

$$\Delta E_c = K (M_i - M_d) \quad (7)$$

where K = a constant proportional to the surface tension, M_i = curvature at the particle's initial position, M_d = curvature at the particle's destination. For incoming particles M_i was set to 0.5 since there is no capillary effect for particles in solution. For particles which would leave the cluster, the capillary effect was included in order to provide a force which stabilises

the cluster. This force accounts for a diffusion influx which is associated with a diffusion gradient that DLA models, due to the sequential release of particles, are unable to take into account.

3. Results

In our initial studies we investigated the role that surface mobility may have on the evolution of aggregate morphology. Fig. 1 shows a typical DLA aggregate consisting of 25 000 particles grown via irreversible precipitation; it demonstrates the highly branched, fractal like morphology reminiscent of DLA-type structures [3,13,22–26]. The introduction of surface mobility and surface tension elements into the model led to a change in the thickening and smoothing of branches of the aggregate (Fig. 2; cf. Fig. 19 in [3]). Each aggregate in Fig. 2 is a

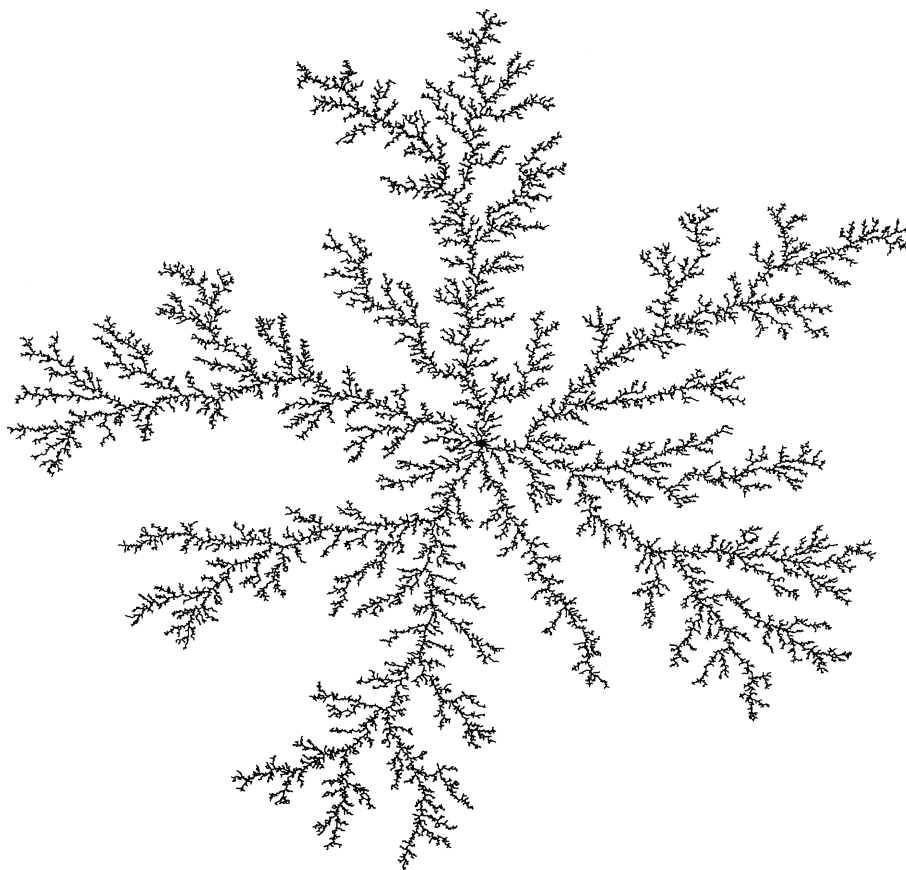


Fig. 1. Typical DLA aggregate consisting of 50 000 particles. Particles are placed on a circular release template of radius $R_{\max} + 100$ (where R_{\max} is the distance of the furthest point of the growing aggregate from its centre) and diffuse until they hit the growing structure, whereupon they adhere.

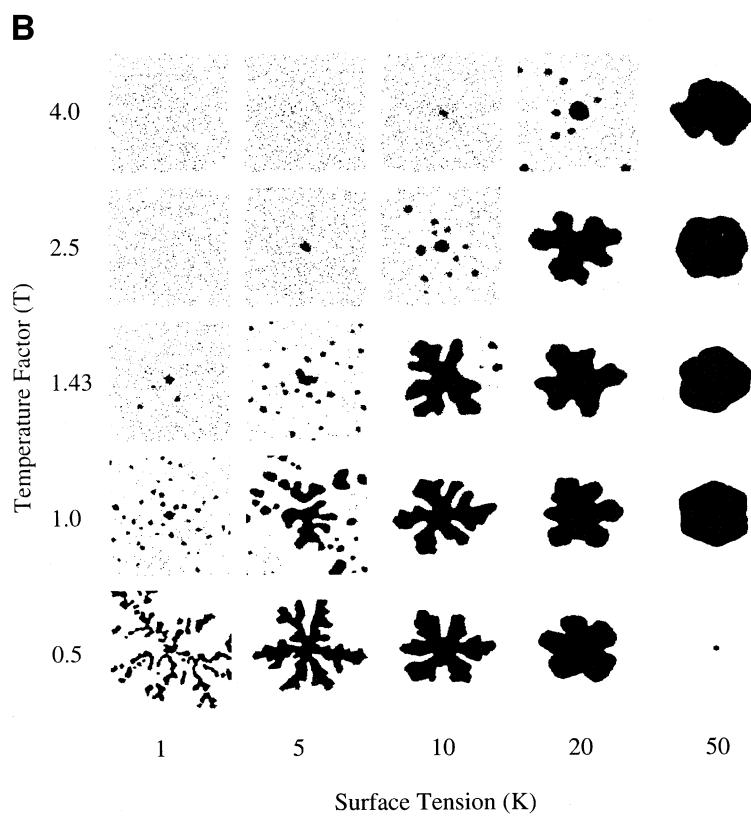
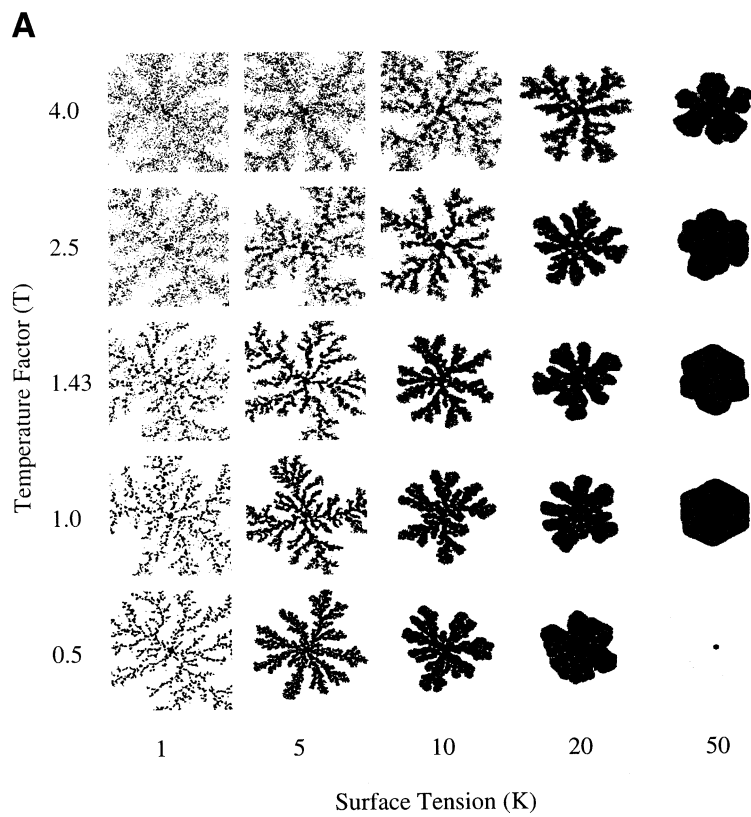
representative simulation with a particular choice of the three parameters: X , K and T . In order to keep the description transparent, the morphology has been described in terms of a T – K plane for three different values of X . This allows direct observations on the influence of temperature, of a surfactant (which will alter K) and of the growth rate (which will alter X).

The variety of patterns obtained may be relatively easily understood. For the largest value of X (Fig. 2A), surface mobility is high and the aggregate has time to reorganise towards a minimum energy profile. For high surface tension, this minimum energy profile tends to minimise the surface. At low temperature the aggregate will tend to be faceted, reflecting the nature of the underlying lattice, whereas as temperature increases there is a corresponding tendency to become rounded. At lower values of surface tension, the cluster shows a tendency towards branching and is more compact when the temperature is increased. At intermediate levels of X (Fig. 2B), surface mobility is lower and the patterns appear to deviate further from equilibrium. The high temperature/surface tension behaviour remains qualitatively the same. However, when surface tension is decreased, the low temperature pattern becomes more and more fractal-like. For a given low surface energy, an increase in temperature leads to the equivalent of the Rayleigh spheroidisation instability [27]: the aggregate splits into droplets. At very high temperature the droplet size becomes under critical and no cluster can be formed. As droplet instability is more difficult for higher surface tensions, this cluster dissolution will be more difficult (i.e., will occur at higher temperature) when the surface tension is higher. For low values of X (Fig. 2C), surface mobility is very low and the patterns deviate even further from equilibrium. For high surface tension and high temperature, the pattern can become sponge-like due to a lack of time for re-organisation (e.g., for $K=20$, $T=0.5$). When surface tension decreases, the patterns become more and more fractal-like. As for previous values of X , high temperatures lead to cluster dissolution. Irrespective of surface mobility, clusters will not form at low temperatures when the surface tension is high, this can be understood using the concept of critical radius for nucleation [28] which scales with the surface tension itself. For very high values of surface tension, this critical radius is large and it

becomes very difficult for incoming particles to attach to the seed, a decrease in temperature will make this process even more difficult.

Fig. 3 shows a range of centric diatom frustules which display a characteristic branching pattern of radiating costae emanating from the centre of the frustule. As noted previously [3], although the introduction of the surface mobility term was able to simulate sintering, those aggregates which did show branching did not have the same degree of regularity as observed in the diatoms shown in Fig. 3. To produce such a regular pattern with amorphous precipitation, diatoms must possess some control mechanism capable of localising the release of new siliceous material. This may involve cytoskeletal elements – e.g., microtubules which have been shown to be associated with the growing periphery of the SDV [12] – which are known to be important in the control of a number of cellular events. The recent discovery of motor proteins (e.g. dynein and kinesin) associated with the intracellular trafficking of vesicles between different organelles [34,35] provides a potential mechanism for the transport of STVs to specific sites of release at the periphery of the SDV. In addition treatment of the diatom *Thalassiosira* with microtubule inhibitors was found to lead to an altered valve morphology [36]. We therefore decided to treat the aggregating environment of our model with some of the characteristics expected for an SDV. Firstly, since the SDV is a closed environment (i.e., silica particles once released into the SDV remain within the SDV), particles in our model were not allowed to move beyond a certain distance (L) of the periphery of the growing aggregate. As the frustule increases in size, the SDV will also increase in size due to the addition of new material to the membrane as STVs become incorporated into its structure. Hence the SDV was simulated to hug the growing precipitate, as suggested by Schmid [36], by using a value of 1 for L .

The next feature to be included into the model was to introduce specific sites of particle release. The number of radiating costae in a frustule is a species dependent trait, but typically ranges from ~ 20 to 50. Two values for the number of distinct sites of release were investigated [24,48], however results from both sets of simulations showed qualitatively similar behaviour, hence only the results for the sim-



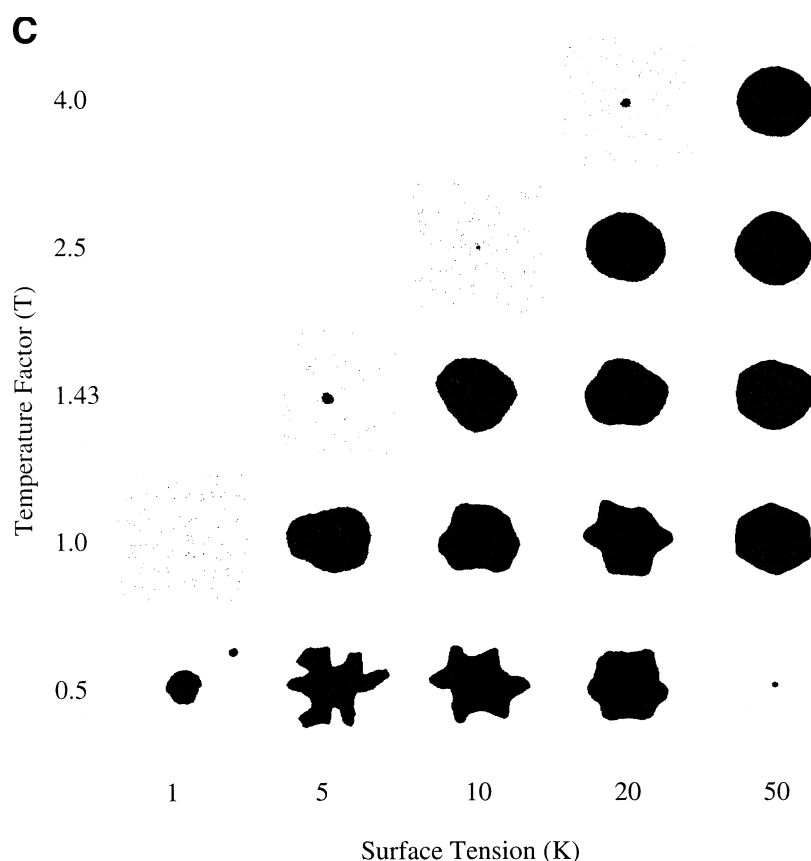


Fig. 2. Morphology maps of aggregates grown using different values of surface tension (K) and temperature (T) factors. The three maps show the effect of growth under conditions of altered surface mobility. (A) $X=0.01$; (B) $X=1.0$; (C) $X=100$. Aggregates consisted of 10000 particles and were grown using a value of 100 for L . Blank spaces indicate that the clusters would not form (see text).

ulations involving 24 sites of release are presented. These sites were initially equally spaced around the release template. As the aggregate increased in size, these sites remained at the same compass positions. New particles were then placed at random on one of these sites. It was initially found that aggregates consisting of only 10000 particles did not reveal the effects of the introduction of specific sites of release (results not shown). Hence for these simulations 50000 particles were used. Simulations were undertaken for two values of X (0.01 and 1.0). Since the amount of time required to perform the simulations scales exponentially with the number of particles used it was not possible to create similar maps for $X=100$.

Fig. 4 shows two morphology maps of aggregates grown with 24 distinct sites of release. Although it should be noted that the morphologies displayed in

Fig. 4 were created with 5 times as many particles as those shown in Fig. 2, in general, the behaviour of these new aggregates with respect to the influence of the three parameters X , K and T , appears to follow that of the aggregates displayed in Fig. 2A,B. For $X=0.01$, surface mobility is very low, and the morphologies are far from equilibrium. Again, due to a lack of re-organisational time, many aggregates display a sponge-like morphology. At the higher level of surface mobility ($X=1.0$), the increase in temperature and decrease in surface tension leads to the similar droplet/dissolution behaviour observed in the earlier simulations. However, it is interesting to note that the aggregates grown with $T=1.43/K=5$, $T=2.5/K=10$ and $T=4/K=20$ in Fig. 4B are much denser than those observed in Fig. 2B. This phenomenon is due to the use of the closed environment of the SDV, leading to an increase in concentration of

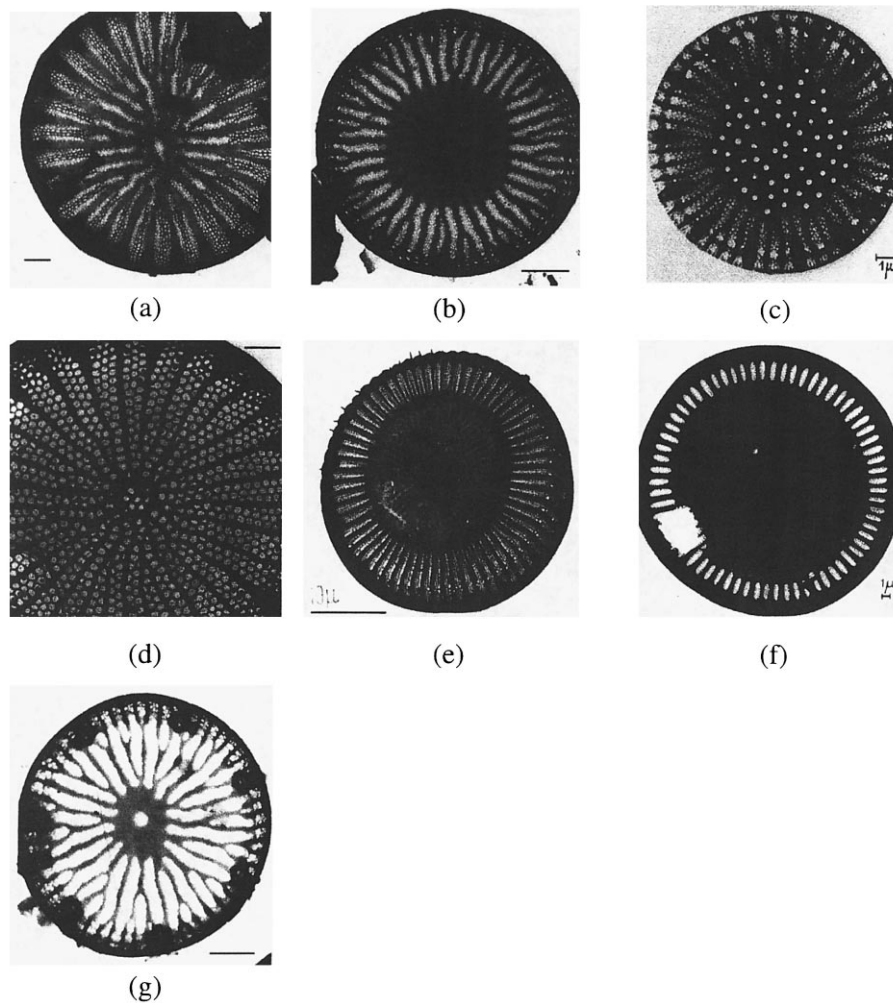
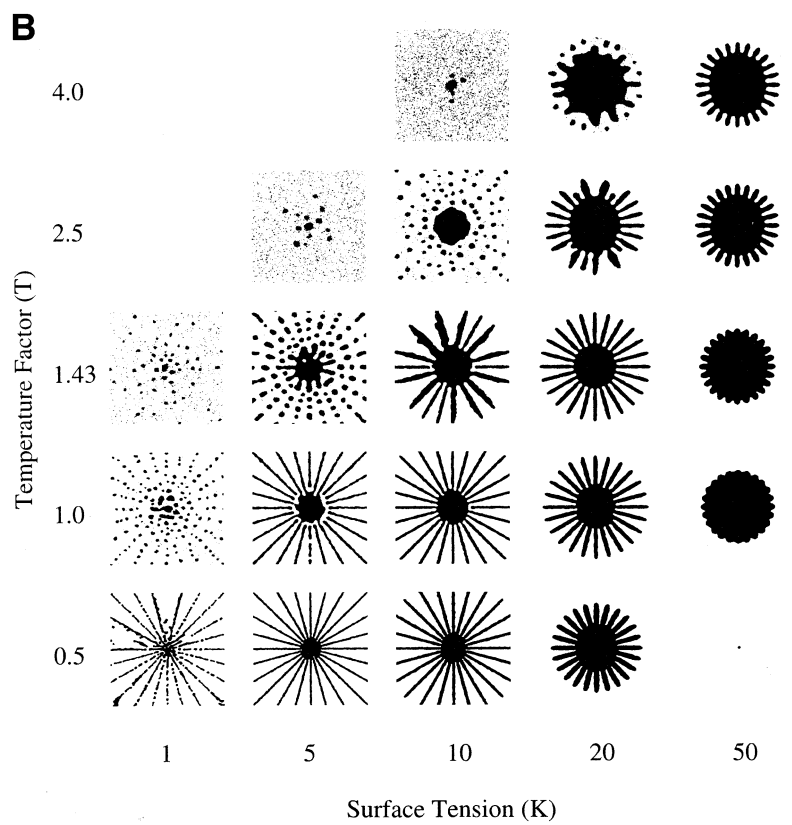
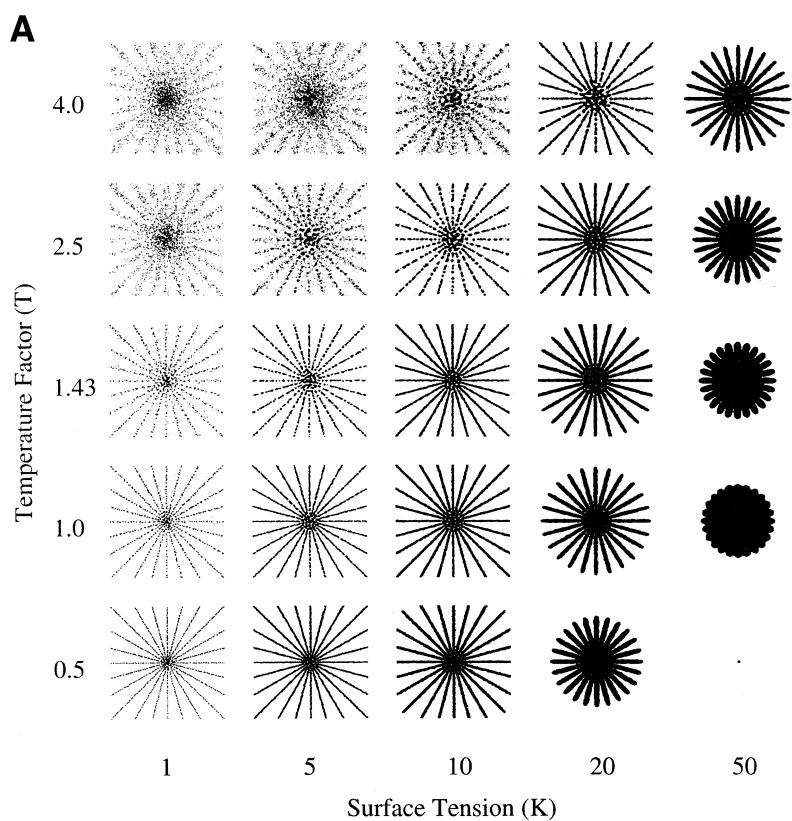


Fig. 3. Typical centric diatom morphologies. (a) *Cyclotella cryptica* (Tafel 738 upper left from [29], with permission, bar = 1 μm); (b) *Cyclotella pseudostelligea* (Tafel 740 upper left from [29], with permission, bar = 1 μm); (c) *Cyclotella comta* (Tafel 23 bottom right from [30], with permission, bar = 1 μm); (d) *Stephanodiscus astraea* (Tafel 315 bottom left from [31], with permission, bar = 1 μm); (e) *Cyclotella meneghiniana* (Tafel 213 bottom left from [32], with permission, bar = 10 μm); (f) *Cyclotella striata* (Tafel 118 top left from [33], with permission, bar = 1 μm); (g) *Cyclotella pseudostelligea*, with 'atypical centre' (Tafel 741 upper right from [29], with permission, bar = 1 μm).

particles. This has the effect of rescaling the surface tension term. Although simulations at very high levels of surface mobility ($X=100$) were not undertaken for reasons mentioned previously, we may assume that the aggregates have enough time between subsequent additions to reorganise towards the energy minima's displayed in Fig. 2C.

The introduction of the distinct sites of release has obviously had a huge influence on the morphogenesis of these aggregates with the formation of radiating branches or islands emanating from their centres. The thickness of these branches is clearly dependent upon both the T and K terms. These results suggest that during diatom morphogenesis, the formation of

Fig. 4. Morphology maps of aggregates grown using 24 specific sites of release for the particles using a range of different values for the surface tension (K) and temperature (T) factors. (A) $X=0.01$; (B) $X=1.0$. The release sites were equally spaced around the release template throughout the simulation. New particles were placed at random on one of these sites. Aggregates consist of 50 000 particles.



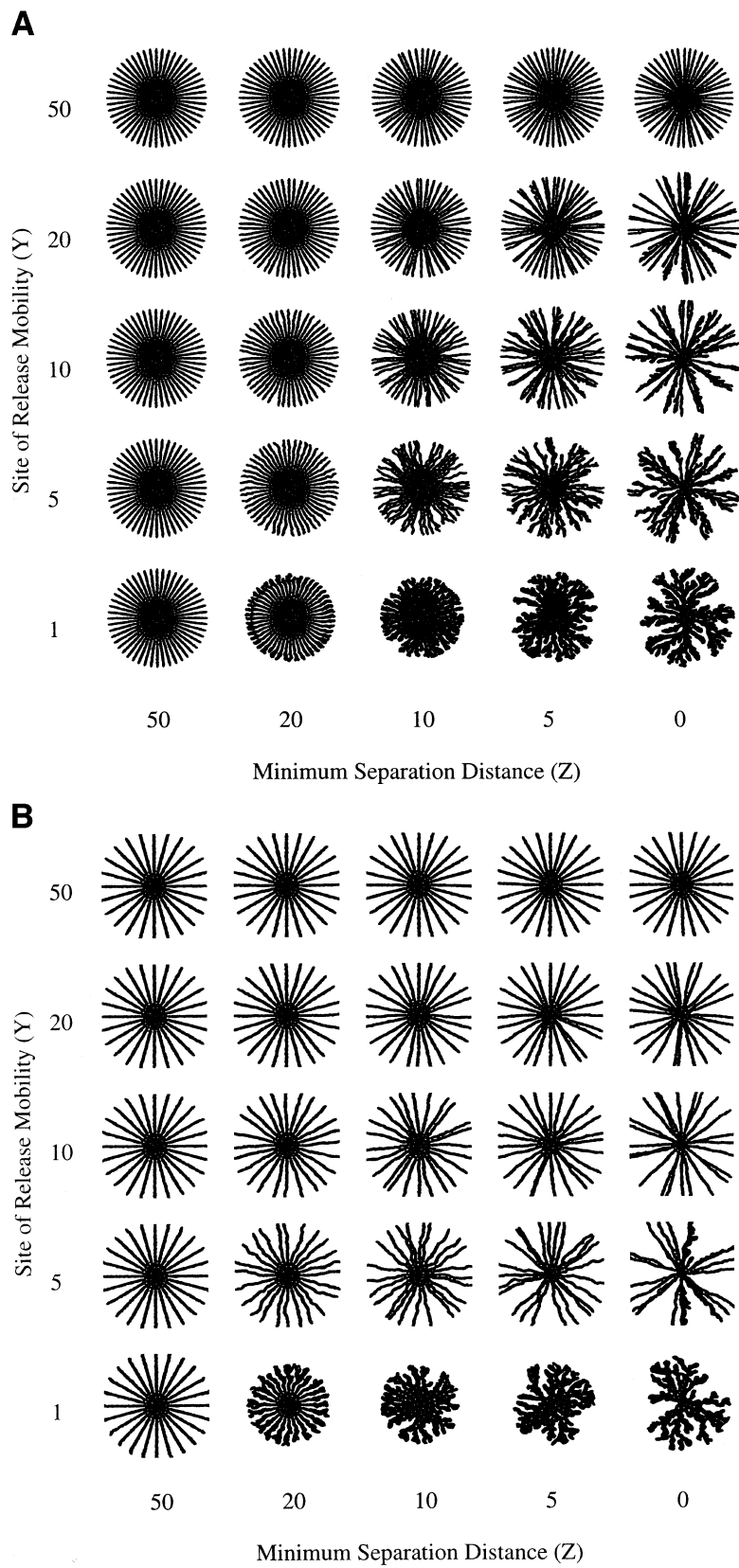


Fig. 5. Morphology maps of aggregates investigating the influence of the amount of movement of the sites of release (Y) and the minimum distance separating two neighbouring sites of release (Z). (A) 24 sites of release: 50 000 particles. (B) 48 sites of release: 100 000 particles. Aggregates were grown with $K=20$, $T=1.43$ and $L=1.0$.

a single costae is associated with a discrete site of deposition. In addition, the thickness of the costae may be dependent upon internal environment of the SDV (concentration of particles, presence of a surfactant, etc.). A number of aggregates (e.g., $X=1.0$, $K=50$, $T=2.5$) display morphologies with a large central mass which evolves branches. These are similar to two of the diatom morphologies shown in Fig. 3. These results suggest that the size of this central mass, which is a species specific trait, is determined by the internal environment of the SDV. Further, at low surface mobilities, holes were found to form within the structures of some aggregates. This suggests that agents within the SDV, capable of reducing the amount of sintering may be responsible for the appearance of pores within certain diatom species. It should be noted that the central mass ('hyaline' region [3]) and the irregular 'pores' it sometimes contains are predictions of the model, and are in no way built into it.

The morphologies shown in Fig. 4 show highly regular patterns of radiating costae. However, certain diatom species do not display such regularity (see Fig. 3g here, and Figs. 1f and 18 in [3]). Such an effect may arise from movement of the site of release during growth of the frustule. To test this hypothesis a number of simulations were undertaken in which the sites of release were given the possibility of movement during the growth of the SDV. This was implemented as outlined in Section 2. Two sets of simulations were investigated, one involving 24 sites of release and one with 48. For the latter set of simulations, in order to resolve some of the morphological features 100 000 particles were used. For each simulation, the same values of X , K and T were used.

Fig. 5 shows morphology maps investigating the roles of the two tunable parameters Y and Z (see Section 2). For both sets of aggregates, it is apparent that a decrease in Y (which leads to an increase in release site mobility) leads to an increase in irregularity in the formation of the branches. The use of a minimum separation distance between two sites of

release also has an effect on branching, with irregular behaviour only being observed after a certain critical size has been attained by the aggregate (e.g., $Y=1$, $Z=20$). Interestingly, a number of aggregates grown with 48 sites of particle release display morphologies in which new branches appear to form. This phenomenon arises since at the beginning of the simulation, the sites of release are very close to each other. It is only when the aggregate attains a certain size that there is space for the sites of release to move apart and exert an individual effect on morphogenesis. This is reflected by the creation of new costae at a certain distance from the aggregate. This distance will depend upon the size of the individual branches. These results demonstrate that the irregularity of branching observed in the costae of certain species of diatoms may be attributable to random fluctuations in the movement of the sites of silica release during frustule formation. In addition, the appearance of new branches, may arise from the unmasking of sites of release which have been present throughout the growth of the frustule. This is an alternative model to sudden branching in centric diatoms, postulated to be due to release of compression by the microfilament ring around the SDV, when the SDV and its nascent valve make a 90° turn at the rim [3].

4. Discussion

In this paper we have presented a novel model system which allows us to take into account the various physical quantities (surface mobility, surface tension and temperature) which may influence the growth pattern of an aggregate. In addition to the simulation of diatom morphogenesis, the model is versatile enough to describe the evolution of morphology in systems as diverse as snowflake transformation [14,15], stability of electrodeposited clusters [16], collagen fibrillogenesis [37] and bacterial colonies [38].

Since the model utilised a circular release boun-

dary for the accreting particles, the main focus of the study was the simulation of the growth of centric diatom frustules. However, by altering the symmetry of the release boundary it would be possible to attempt to simulate other types of diatoms such as pennates. Previous models of DLA have led to the formation of highly branched fractal-like aggregates. Here, surface mobility was introduced to simulate the mechanism of sintering thought to be responsible for the smoothing of the branch surface [8]. Although surface mobility has previously been included in models of diatom morphogenesis [3,39], the method utilised in this study provides a more rigorous and amenable examination of the mechanisms controlling the evolution of morphology.

A somewhat surprising result was the spontaneous appearance of pores within the structure of the aggregate due to a lack of reorganisational time. Trapped holes have been observed in previous simulations but were not commented upon (Figs. 19–21 in [3]). It has previously been suggested that the formation of pores within diatom frustules occurs via the formation of spacer vesicles within the mother liquor [40]. The results from our simulations suggest an alternative mechanism. During frustule growth, a surface stabilising element is introduced within the SDV. This has the effect of reducing the period of surface relocalisation and fixing the particles in position and hence trapping any pores contained within the structure.

The production of aggregates with regular branched morphologies suggests that the growth of the primary costae in diatoms may be associated with the deposition of new material at specific points on the perimeter of the SDV, the width of the costae being dependent upon both temperature and surface tension factors, the latter being controlled by the environment of the SDV. Indeed studies by Iler [7] on the aggregation of silica have shown that the changes in salinity and pH can have a marked effect on precipitation. In addition, other studies have shown that a higher saline environment can lead to the formation of aberrant frustules which contain lower amounts of silica than those grown under low saline conditions [9,10]. The results from our model thus strongly support the theory that it is the nature of the chemical environment within the SDV (which may be a species specific trait, sensitive

to the local environment) which is responsible for the determination of many features of the diatom frustule.

Since each costae is associated with a distinct site of release, the numbers of primary costae will be dependent upon the numbers of release sites which may also be a species specific trait. At present we can only speculate on the mechanism underlying the release of new siliceous material to specific sites on the SDV. However, given their association with the periphery of the SDV [12], it is possible that such a mechanism involves the use of microtubules.

During initial stages of frustule growth, the centrosome of the microtubule array is located near the centre of the SDV membrane. Microtubules originating from this centre would thus form a radial array extending over the surface of the SDV. This offers the possibility that the microtubules serve as guides for the transport of the STVs. In such a model, during growth of the frustule, STVs move along microtubules until they reach the periphery of the growing SDV (cf. the analogous movement of pigment granules in melanophores [41]). The STV then fuses with the membrane of the SDV, releasing its contents into the interior. The formation of each costae is then associated with an individual microtubule. The formation of new branches during growth may then be attributable to the divergence of two closely associated microtubules in a bundle (for a review of microtubule bundling see [42]), as observed for certain aggregates in Fig. 5B.

The involvement of microtubules is based upon two premises; firstly they must be stable for at least the time of frustule growth and secondly that STVs travel along their length and are released only at the periphery of the SDV. Although the stability of microtubules can be species specific, they are typically stable for 10–20 min [43] which is approximately the time it takes for the first stage of valve formation (prior to thickening) [3]. The trafficking of STVs along the length of a microtubule, could then be accounted for by the involvement of motor proteins, such as dynein and kinesin, which have been implicated in a number of secretory processes [34,35]. The polarity in movement demonstrated by such proteins [44] provides a mechanism to ensure that the STVs move towards the periphery of the SDV. The directed release of the STVs at the periphery of the

SDV may then involve either ion gradients, which may regulate the attachment of the motor proteins to the microtubule [34,45], or additional proteins which may link the microtubule to the membrane of the SDV and act as receptors for the STVs [46,47]. The latter possibility is analogous to the transport of neurotransmitter containing vesicles by microtubules to synapses, where they fuse with the plasmalemma and release their contents [48].

Indeed, the presence of STV receptors at the periphery of the SDV membrane provides an alternative mechanism for the directed release of silica. During growth of the frustule STVs could diffuse at random through the cytoplasm until they encounter one of these receptors, whereupon they associate with the SDV and release their contents. The use of receptors also provides a potential mechanism for branching. In addition to their siliceous cargo, the membrane of the STVs which fuses with the membrane of the SDV may also contain new receptors. If receptors are being used by the diatom to localise deposition of new material, there needs to be an additional mechanism controlling the position of these receptors within the SDV membrane. This could involve their attachment to the radially distributed pattern of microtubules postulated above. An investigation into the possible role of receptors requires an analysis of the contents of the SDV membrane. However, although it has been possible to isolate proteins associated with the frustule itself [49], such an analysis is hampered by an inability to isolate the SDV.

It should be noted that it was not the purpose of this model to simulate every aspect of diatom frustule formation. However, it could be extended to investigate other features of diatoms such as the secondary thickening of costae in the third dimension after the initial growth of the frustule (reviewed in [3]). This process may involve the use of two populations of STVs, in which the initial population is localised to distinct sites on the SDV membrane. The second population of STVs are not targeted by the cell and hence diffuse within the cytoplasm until they encounter any part of the SDV ('face arrivals', Fig. 14 in [3]). The two populations may contain different sizes of silica particles, which may alter the finer morphological features of the frustule. Such features, amongst others, could be introduced

into the model of diatom morphogenesis and would further our understanding of the process of diatom frustule formation and begin to allow us to understand exactly what is different between species in the silica precipitation process.

Two classes of centric diatoms have costal patterns that still evade us, in terms of plausible computer simulations. One is *Thalassiosira eccentrica* exhibiting parallel bundles of costae. Most of the costae in a bundle or 'domain' (an analogy to microcrystallinity: Fig. 1g in [3]) do not project back to the centre of the valve. The other pattern that needs simulation is the honeycomb or hexagonal lattice. While this probably derives from a branching pattern [3,50], how, at least in some cases, an almost perfect hexagonal arrangement is achieved, remains an open problem. The postulated flexibility of thin strands of just precipitated silica as a component of the process [3] goes beyond DLA modelling.

Acknowledgements

One of the authors (J.P.) would like to thank the Royal Society for providing support in the form of a NATO postdoctoral fellowship.

References

- [1] D. Werner, *The Biology of Diatoms*, University of California Press, Berkeley, 1977.
- [2] F.E. Round, R.M. Crawford, D.G. Mann, *The Diatoms, Biology and Morphology of the Genera*, Cambridge University Press, Cambridge, 1990.
- [3] R. Gordon, R.W. Drum, *Int. Rev. Cytol.* 150 (1994) 243–372.
- [4] A.M.M. Schmid, D. Shultz, *Protoplasma* 100 (1979) 267–288.
- [5] L.H. Allen, E. Matijevic, *J. Colloid Interface Sci.* 31 (1969) 287–296.
- [6] P.W. Voorhees, *J. Stat. Phys.* 38 (1985) 231–252.
- [7] R.K. Iler, *The Chemistry of Silica: Solubility, Polymerization, Colloid and Surface Properties, and Biochemistry*, John Wiley and Sons, New York, 1979.
- [8] L. Righetto, A. Polissi, D. Comi, B. Marcandalli, I.R. Bellobono, G. Bidoglio, *Ann. Chim.* 77 (1987) 437–455.
- [9] M.L. Tuchman, E. Theriot, E.F. Stoermer, *Arch. Protistenk.* 128 (1984) 319–326.
- [10] D.J. Conley, S.S. Kilham, E. Theriot, *Limnol. Oceanogr.* 34 (1989) 205–213.

- [11] H.R. Preisig, *Protoplasma* 181 (1994) 29–42.
- [12] J. Pickett-Heaps, A.M.M. Schmid, L.A. Edgar, in: F.E. Round, D.J. Chapman (Eds.), *Progress in Phycological Research*, Biopress, 1990.
- [13] R. Gordon, *Fed. Proc.* 40 (1981) 827.
- [14] J. Nittmann, H.E. Stanley, *Nature* 321 (1986) 663–668.
- [15] J. Nittmann, H.E. Stanley, *J. Phys. A* 20 (1987) L1185–L1191.
- [16] M. Matsushita, M. Sano, Y. Hayakawa, H. Honjo, Y. Sawada, *Phys. Rev. Lett.* 53 (1984) 286–289.
- [17] J.G. Masek, D.L. Turcotte, *Earth Plan. Sci. Lett.* 119 (1993) 379–386.
- [18] J. Coombs, J.A. Lauritis, W.M. Darley, B.E. Volcani, *Z. Pflanzenphysiol.* 59 (1968) 274–284.
- [19] R. Gordon, *J. Chem. Phys.* 48 (1968) 1408–1409.
- [20] R. Gordon, in: G. Karreman (Ed.), *Cooperative Phenomena in Biology*, Pergamon Press, New York, 1980, pp. 189–241+errata.
- [21] J. Rowlinson, B. Widom, *Molecular Theory of Capillarity*, Oxford University Press, Oxford, 1984.
- [22] R. Julien, R. Botet, *Aggregation and Fractal Aggregates*, World Scientific, Singapore, 1987.
- [23] J. Feder, *Fractals*, Plenum, New York, 1988.
- [24] T. Vicsek, *Fractal Growth Phenomena* (2nd ed.), World Scientific, Singapore, 1992.
- [25] K.S. Birdi, *Fractals in Chemistry, Geochemistry and Biophysics*, Plenum, New York, 1993.
- [26] J.A. Kaandorp, *Fractal Modelling: Growth and Form in Biology*, Springer, Berlin, 1994.
- [27] F.A. Nichols, W.W. Mullins, *J. Appl. Phys.* 36 (1963) 1826–1836.
- [28] W.A. Tiller, *The Science of Crystallisation*, Cambridge University Press, Cambridge, 1991.
- [29] J. Gerloff, J.G. Helmcke, in: J.G. Helmcke, W. Krieger, J. Gerloff (Eds.), *Diatomeenschalen im elektronenmikroskopischen Bild*, vol. 8, J. Cramer, Lehre, 1974.
- [30] J.G. Helmcke, W. Krieger, in: J.G. Helmcke, W. Krieger (Eds.), *Diatomeenschalen im elektronenmikroskopischen Bild*, vol. 1, J. Cramer, Weinheim, 1962.
- [31] U. Geissler, J. Gerloff, J.G. Helmcke, W. Krieger, B. Reimann, in: J.G. Helmcke, W. Krieger (Eds.), *Diatomeenschalen im elektronenmikroskopischen Bild*, vol. 4, J. Cramer, Weinheim, 1963.
- [32] U. Geissler, J. Gerloff, J.G. Helmcke, W. Krieger, B. Reimann, in: J.G. Helmcke, W. Krieger (Eds.), *Diatomeenschalen im elektronenmikroskopischen Bild*, vol. 3, J. Cramer, Weinheim, 1961.
- [33] J.G. Helmcke, W. Krieger, in: J.G. Helmcke, W. Krieger (Eds.), *Diatomeenschalen im elektronenmikroskopischen Bild*, vol. 2, J. Cramer, Weinheim, 1962.
- [34] N.B. Cole, J. Lippincott-Schwartz, *Curr. Opin. Cell Biol.* 7 (1995) 55–64.
- [35] M.P. Sheetz, *Cell Struct. Funct.* 21 (1996) 369–373.
- [36] A.M.M. Schmid, in: D.G. Mann (Ed.), *Proceedings of the 7th International Symposium on Living and Fossil Diatoms*, O. Koeltz, Koenigstein, Germany, 1984.
- [37] J. Parkinson, K.E. Kadler, A. Brass, *J. Mol. Biol.* 247 (1995) 823–831.
- [38] E. Ben-Jacob, O. Shochet, A. Tenenbaum, I. Cohen, A. Czirok, T. Vicsek, *Nature* 368 (1994) 46–49.
- [39] R. Gordon, B.D. Aguda, in: *Proceedings of the Annual International Conference of the IEEE Engineering in Medicine and Biology Society*, part 1/4: Cardiology and Imaging, Institute of Electrical and Electronics Engineers, New York, 1988, pp. 273–274.
- [40] A.M.M. Schmid, *Protoplasma* 181 (1994) 43–60.
- [41] V.I. Rodionov, G.G. Borisy, *Nature* 386 (1997) 170–173.
- [42] R. Gordon, *The Hierarchical Genome and Differentiation Waves: Novel Unification of Development, Genetics and Evolution*, 2 vols., World Scientific, Singapore, and Imperial College Press, London, 1999.
- [43] R. Pepperkok, M.H. Bre, J. Davoust, T.E. Kreis, *J. Cell Biol.* 111 (1990) 3003–3012.
- [44] S.A. Endow, K.W. Waligora, *Science* 281 (1998) 1200–1202.
- [45] G.Q. Bi, R.L. Morris, G.C. Liao, J.M. Alderton, J.M. Scholey, R.A. Steinhardt, *J. Cell Biol.* 138 (1997) 999–1008.
- [46] E. Mandelkow, E.-M. Mandelkow, *Curr. Opin. Cell Biol.* 7 (1995) 72–81.
- [47] F. Rajas, V. Gire, B. Rousset, *J. Biol. Chem.* 271 (1996) 29882–29890.
- [48] J.G. Hanley, P. Koulen, F. Bedford, P.R. GordonWeeks, S.J. Moss, *Nature* 397 (1999) 66–69.
- [49] N. Kroger, G. Lehmann, R. Rachel, M. Sumper, *Eur. J. Biochem.* 250 (1997) 99–105.
- [50] G.A. Fryxell, G.R. Hasle, *Nova Hedwigia* 54 (Suppl.) (1977) 67–98.